



Search for top quark production via flavor-changing neutral currents at CDF

The CDF Collaboration
URL <http://www-cdf.fnal.gov>
(Dated: October 25, 2008)

We report on a search for single top-quark production via flavor-changing neutral currents (FCNC) in the process $u(c) + g \rightarrow t$ using $p\bar{p}$ collision data collected by the Collider Detector at Fermilab at $\sqrt{s} = 1.96$ TeV. The analyzed data set corresponds to an integrated luminosity of 2.2 fb^{-1} . Selected candidate events feature exactly one isolated electron or muon with high transverse momentum, missing transverse energy, and exactly one hadronic jet which has been identified to originate from a b quark. Candidate events are classified as signal-like or background-like by a neural network trained on simulated events. The distribution of the neural network discriminant is fitted to template distributions of signal and background events. We find good agreement of the observed distribution with the one predicted by the standard model and thus no evidence for FCNC top quark production. Therefore, we set an upper limit on the production cross section $\sigma(u(c) + g \rightarrow t) < 1.8 \text{ pb}$ at the 95% confidence level (C.L.). Using theoretical predictions we convert the cross section limit in upper limits on the anomalous coupling parameters κ_{gtu}/Λ and κ_{tcg}/Λ , where κ_{gtu} and κ_{tcg} define the strength of the gtu and tcg couplings and Λ defines the scale of new physics. The derived limits at the 95% C.L. are: $\kappa_{gtu}/\Lambda < 0.018 \text{ TeV}^{-1}$ and $\kappa_{gtc}/\Lambda < 0.069 \text{ TeV}^{-1}$. These results constitute an improvement of 50% over existing upper bounds.

I. INTRODUCTION

In the standard model (SM) of particle physics flavor-changing neutral currents (FCNC) are absent at tree level, but occur only at higher order in perturbation theory through loop diagrams. These radiative corrections are further suppressed through the GIM mechanism [1], which induces a cancellation of Feynman diagrams involving different quark flavors in the quantum loops. In the case of fully degenerate up-type and down-type quark masses the cancellation would be perfect. In bottom-quark decays the large top-quark mass alleviates the GIM-suppression leading to FCNC decays with branching ratios (BR) at the level of 10^{-6} , while in top-quark sector FCNC decays are much stronger suppressed and occur only at the order of $\text{BR} \approx 10^{-10}$ to 10^{-14} [2]. Any evidence for FCNC will therefore be a signal of new physics beyond the SM. Enhanced FCNC couplings can be realized in extensions of the standard theory, such as models with multiple Higgs doublets [2–4], supersymmetric models with R-parity violation [5, 6], or topcolor-assisted technicolor theories [7]. In certain regions of parameter space of these models the BRs of FCNC decays can reach levels of 10^{-3} to 10^{-5} . But even this tremendous enhancement renders the detection of FCNC top-quark decays a very challenging task at the Tevatron, first because one can only expect to reconstruct a few top-quarks in these modes, and second because the backgrounds for the most promising mode, $t \rightarrow cg$ is rather difficult. Therefore, it has been suggested to search for FCNC couplings in top-quark production, rather than top-quark decay [8–12].

In this note we present a search for the non-SM single top-quark production processes $u(c) + g \rightarrow t$. We do not consider a particular model, but perform a model-independent search based on an effective theory [8, 9] that contains additional flavor-changing operators in the Lagrangian

$$g_s \frac{\kappa_{gtu}}{\Lambda} \bar{u} \sigma^{\mu\nu} \frac{\lambda^a}{2} t G_{\mu\nu}^a + h.c. \quad (1)$$

where κ_{gtu} is a dimensionless parameter that relates the strength of the new, anomalous coupling to the strong coupling constant g_s and Λ is the new physics scale, related to the mass cut-off above which the effective theory breaks down. The gluon field tensor is denoted $G_{\mu\nu}^a$, the λ^a are the Gell-Mann matrices, and $\sigma^{\mu\nu} \equiv \frac{i}{2}[\gamma^\mu, \gamma^\nu]$ transforms as a tensor under the Lorentz group. The analogous expression to (1) for the gtc coupling is implied. The existence of FCNC operators implies the production of top quarks via $u(c) + g \rightarrow t$, but also non-SM decays $t \rightarrow u(c) + g$. In the allowed parameter space for κ_{gtu} and κ_{gtc} one is met with an experimentally favourable situation: while the FCNC production cross section of single top-quarks is considerably large, in the range of several pb, the BR into FCNC decays is very small, and top-quarks can thus be reconstructed in the SM decay mode $t \rightarrow Wb$. Our analysis is the first one at the Tevatron searching for the $2 \rightarrow 1$ processes $u(c) + g \rightarrow t$, while a previous analysis [13] by the DØ collaboration has looked for $2 \rightarrow 2$ processes, such as $q\bar{q} \rightarrow t\bar{u}$, $ug \rightarrow tg$, and $gg \rightarrow t\bar{u}$, resulting in the best upper limits on the anomalous gtu and gtc couplings to date: $\kappa_{gtu}/\Lambda < 0.037 \text{ TeV}^{-1}$ and $\kappa_{gtc}/\Lambda < 0.15 \text{ TeV}^{-1}$ at the 95% C.L.. FCNC couplings to the top-quark involving the photon or Z boson have been constrained by the analysis of top-quark decays at the Tevatron [14], the search for $e^+e^- \rightarrow t\bar{c}/t\bar{u}$ reactions at LEP by the L3 collaboration [15], and the search for $ep \rightarrow e + t + X$ reactions at HERA [16, 17].

II. EVENT SELECTION

We select a set of candidate events in the $W + 1$ jet topology, $t \rightarrow W^+b \rightarrow \ell\nu b$, by requiring exactly one isolated electron candidate with $E_T > 20 \text{ GeV}$ or one identified muon with $p_T > 20 \text{ GeV}/c$, $\cancel{E}_T > 25 \text{ GeV}$ consistent with a neutrino from W decay, and exactly one hadronic jet with $|\eta| \leq 2.8$ and $E_T > 20 \text{ GeV}$ [19]. The jets are clustered in fixed cones of a radius $\Delta R = \sqrt{(\delta\eta)^2 + (\Delta\phi)^2} = 0.4$ and the jet energies are corrected for instrumental detector effects [20]. The hadronic jet is further required to contain a reconstructed secondary vertex consistent with the decay of a b hadron [21]. In order to reduce the Z +jets, $t\bar{t}$ and diboson backgrounds, candidate events with a second lepton are rejected. Cosmic rays are identified using timing and track displacement information and are removed, as are photon conversion candidates. Multijet backgrounds without a leptonic W decay (“non- W ” events) are minimized with requirements on e.g., the angle between the direction of \cancel{E}_T and other objects in the event. Our event selection is identical to the one used for the measurement of standard model single top-quark production [22] except for the requirement on the number of jets. Based on the selection criteria outlined above we observe 2472 candidate events.

III. MONTE CARLO SAMPLES AND BACKGROUND ESTIMATE

The diboson processes WW , WZ , ZZ , and $t\bar{t}$ event yields are predicted using PYTHIA [23] Monte Carlo samples, normalized to NLO cross sections [24, 25]. Standard model single top-quark rates are estimated with simulated events

TABLE I: Background composition and predicted number of $W+1$ jet events in 2.2 fb^{-1} of CDF Run II data.

Process	ν
$Wb\bar{b}/Wc\bar{c}$	750.9 ± 225.3
Wc	622.3 ± 186.7
Wjj	769.9 ± 100.5
$t\bar{t}$	12.3 ± 1.8
non- W	43.0 ± 17.2
Diboson	19.9 ± 2.0
Z +jets	26.6 ± 4.2
SM single-top	24.4 ± 3.6
Total prediction	2269.3 ± 434.3
Observed	2472

from tree-level matrix-element generator MADEVENT [26], subsequent showering with PYTHIA, and normalization to NLO cross sections [27]. The processes with vector bosons (W or Z) and jets are generated with ALPGEN [28], with parton showering and underlying event simulated with PYTHIA. A normalization factor of 1.4 ± 0.4 is required to match ALPGEN's prediction for the fraction of $Wb\bar{b}$ and $Wc\bar{c}$ events. The contribution from events with mistakenly tagged light-flavor jets (Wjj) is estimated by measuring the rate of such mistags in generic jet data as a function of the jet's E_T , η , track multiplicity, number of vertices, position of the primary vertex and the total transverse energy in the event [21]. The mistag rate is then applied to the $W+1$ jet candidate sample before b -tagging. The total contribution is corrected for diboson, $t\bar{t}$, non- W and $Wb\bar{b}+Wc\bar{c}+Wc$ events. Multi-jet non- W events typically have less missing transverse energy than events containing W bosons. By using a data-derived non- W model and a W +jets Monte Carlo model we fit the \cancel{E}_T distribution and extract the non- W fraction in the high \cancel{E}_T signal region. Using the described compound model of simulated events, theoretical cross sections and normalizations in side-band regions we predict the composition of the $W+1$ jet data set as given in Table I. Top-quark events created via the processes $u(c) + g \rightarrow t$ are simulated using the matrix-element generator TOPREX [29] followed by parton showering with PYTHIA. For the event generation, the coupling constants have been chosen to yield a cross section of 1 pb, but it has been verified that the event kinematics does not depend on the choice of these parameters within the range relevant for our analysis. For an FCNC top-quark cross section of 1 pb we expect a yield of 35.3 ± 5.3 events.

IV. NETWORK TRAINING AND INPUT VARIABLES

As in the case of the SM single top-quark search the large background in the $W+1$ jet data set calls for the use of multivariate techniques and we employ the same technology as the neural network analysis reported in ref. [22, 31]. Neural networks (NN) have the general advantage that correlations between the discriminating input variables are identified and utilized to optimize the separation power between signal and background. The networks are developed using the NEUROBAYES analysis package [30] which combines a three-layer feed-forward neural network with a complex and robust preprocessing of the input variables. Bayesian regularization techniques are utilized to avoid over-training. The network infrastructure consists of one input node for each input variable plus one bias node, an arbitrary number of hidden nodes, and one output node which gives a continuous output in the interval $[-1, 1]$. We train the NN on the samples of simulated events listed above using a mixture of 50% signal events versus 50% background events. The background composition is chosen in the proportions as stated in Table I. Three categories of input variables are considered for the NN training: variables directly derived from the physics objects, variables derived from kinematic reconstruction of the event, and variables calculated by advanced algorithms. In total, 21 variables were considered, but only those 14 were kept that show a significance larger than three standard deviations in discriminating signal and background. These variables of the first category are: the transverse momentum and the pseudorapidity of the charged lepton, $p_{T,\ell}$ and η_ℓ , the transverse momentum of the b -quark jet, $p_{T,b}$, the difference in azimuth angle between the jet and $\vec{\cancel{E}}_T$, $\Delta\phi(j, \vec{\cancel{E}}_T)$, and between lepton and $\vec{\cancel{E}}_T$, $\Delta\phi(\ell, \vec{\cancel{E}}_T)$, and the distance in the η - ϕ plane between the charged lepton and the jet, $\Delta R(\ell, j)$. The W boson candidate is reconstructed in its leptonic decay mode from the charged lepton and $\vec{\cancel{E}}_T$ applying the kinematical constraint $M_{\ell\nu} = M_W$. The two-fold ambiguity for the z -component of the neutrino momentum is solved by choosing the smallest $|p_{z,\nu}|$ solution. Based on W boson reconstruction we define two input variables: $M_{T,\ell\nu}$ and $\eta_{\ell\nu}$. We further reconstruct top-quark candidates by adding the b -quark jet to the reconstructed W boson and thereby define the following input variables: $M_{\ell\nu b}$, $M_{T,\ell\nu b}$, the rapidity $y_{\ell\nu b}$, and

$Q_\ell \cdot \eta_{\ell\nu b}$, where Q_ℓ is the charge of the lepton. Some of the important input variables are shown in Fig. 1.

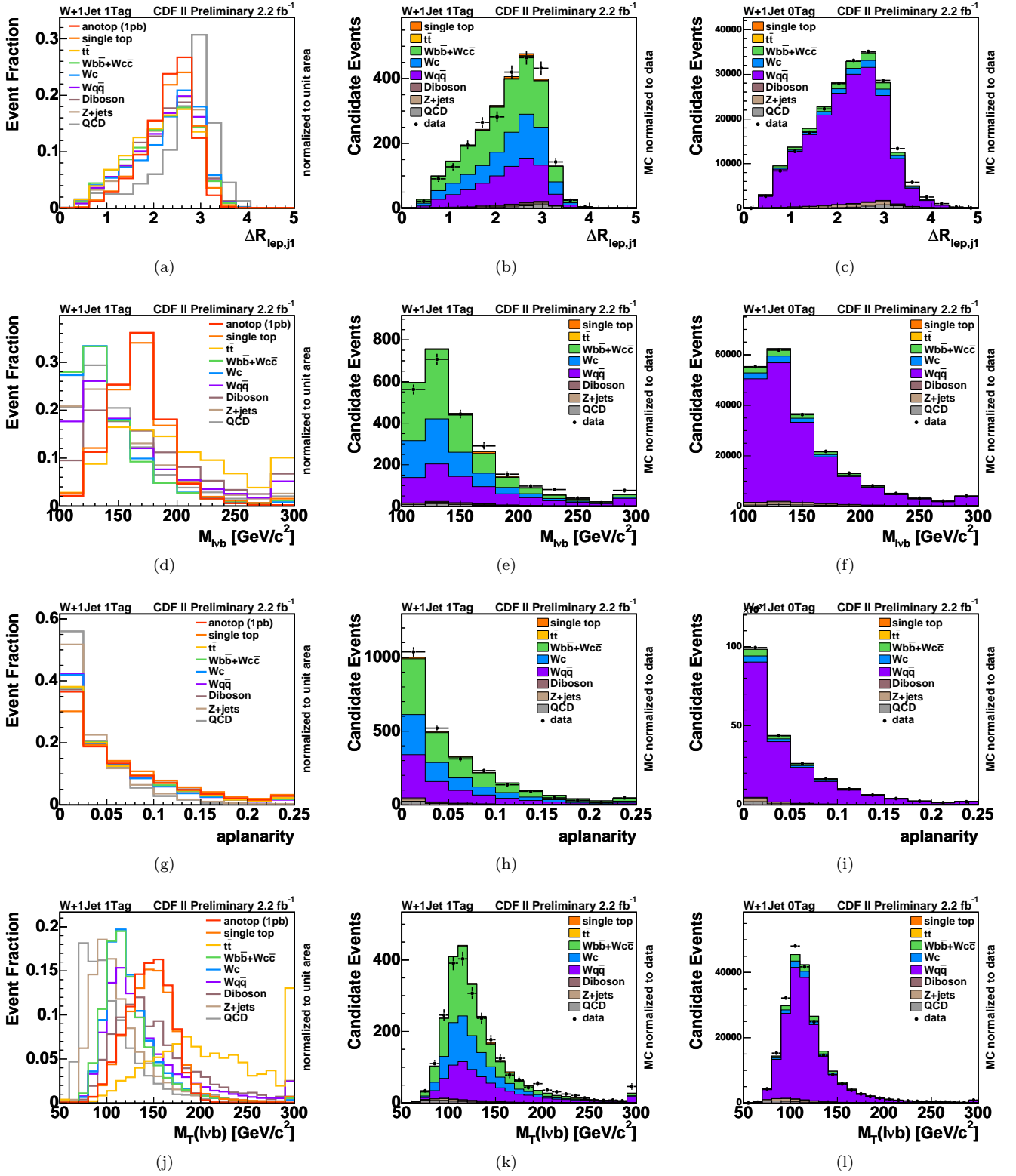


FIG. 1: Some of the variables with the highest discriminating ability used for the neural network analysis. On the left signal and background shapes, in the middle data compared to Monte Carlo and on the right a check for the background shapes in the $W + 1$ jet zero tag.

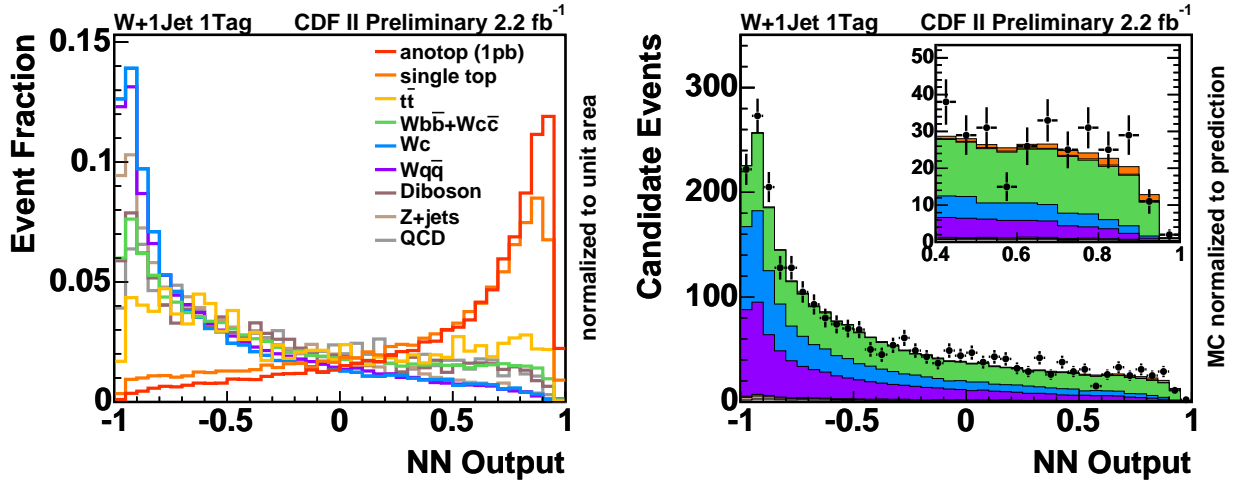


FIG. 2: Distribution of the NN discriminant. (a) Discriminant shapes for the different physics processes normalized to unit area. (b) The composite model is compared to the distribution observed in collision data.

An additional input variable is the output of an advanced jet flavor separating tool mainly developed to increase the sensitivity of the standard model single top-quark searches [31]. The flavor separator is also based on a NN which employs 31 input variables to discriminate b -quark jets on one hand from c -quark jets and light-quark jets on the other hand. To describe the event shape in general we use the aplanarity which is defined by $\frac{3}{2}$ of the smallest eigenvalue of the momentum tensor constructed from the b -quark jet, the charged lepton and the reconstructed neutrino.

V. MEASUREMENT

We apply the NN to the samples of simulated events and obtain template distributions of the network output for all physics processes considered. These templates are weighted by their expected event yield and the resulting composite model is compared to the NN output distribution observed in collision data in Fig. 2. For this comparison the $Wb\bar{b}/Wc\bar{c}$ and Wc event rates were scaled by factors obtained from a fit to the jet flavor separator distribution.

To measure the potential content of FCNC produced single top-quarks in the observed data set we perform a binned maximum likelihood fit of the NN output distribution. The effect of systematic uncertainties are parametrized in the likelihood function including the correlation of rate normalization effects (Tables II and III) and shape distortions of the template distributions (Fig. 3). Uncertainties in the jet energy scale, b -tagging efficiencies, lepton identification and trigger efficiencies, the amount of initial and final state radiation, PDFs, factorization and renormalization scale dependence and Monte Carlo modeling have been explored and incorporated in this analysis.

Source	anoTop	single-top	tt	diboson	Z+jets
ISR less/more	2.8/-3.9 %	1.2/-0.7 %	-0.7/-6.3 %		
FSR less/more	0.1/1.0 %	0.9/2.0 %	-6.5/-1.6 %		
IFSR less/more	2.9/-2.9 %	2.1/1.3 %	-7.2/-7.9 %		
PDF	3.4/-3.7 %	2.8/-3.0 %	1.9/-2.3 %		
ϵ_{evt}	13.7/-13.7 %	5.7/-5.7 %	2.4/-2.4 %	7.8/-7.8 %	10.2/-10.2 %
Luminosity	6.0/-6.0 %	6.0/-6.0 %	6.0/-6.0 %	6.0/-6.0 %	6.0/-6.0 %
Cross section uncertainties	0.0 %	12.6/-12.6 %	12.4/-12.4 %	1.9/-1.9 %	10.8/-10.8 %
M_{top} 172/178	5.3/-4.8 %	6.1/-5.5 %	9.7/-8.9 %		

TABLE II: Systematic rate uncertainties for 1 jet and 1 b tag

All parameters describing systematic uncertainties in the likelihood function are integrated out using Gaussian integration kernels. The Gaussian constraints are given in Table IV.

Applying a prior probability density, which is 0 if the FCNC cross section σ_t is negative and 1 if $\sigma_t \geq 0$ pb, we obtain the posterior probability density $p(\sigma_t)$. No significant rate of single top-quarks produced by FCNC is observed and we set an upper limit on the cross section of 1.8 pb at the 95% C.L. which is in good agreement with the expected

process	1jet 1tag
ano-top	-6.7/-2.2 %
single-top	-9.6/+10.0 %
$t\bar{t}$	-15.6/+18.8 %
$Wb\bar{b}$	-9.3/+8.7 %
$Wc\bar{c} + Wc$	-6.3/+7.4 %
Z+jets	-0.1/+0.1 %
Diboson	-11.5/+13.5 %
Mistags	-0.1/+0.1 %

TABLE III: Systematic JES down/up rate uncertainties

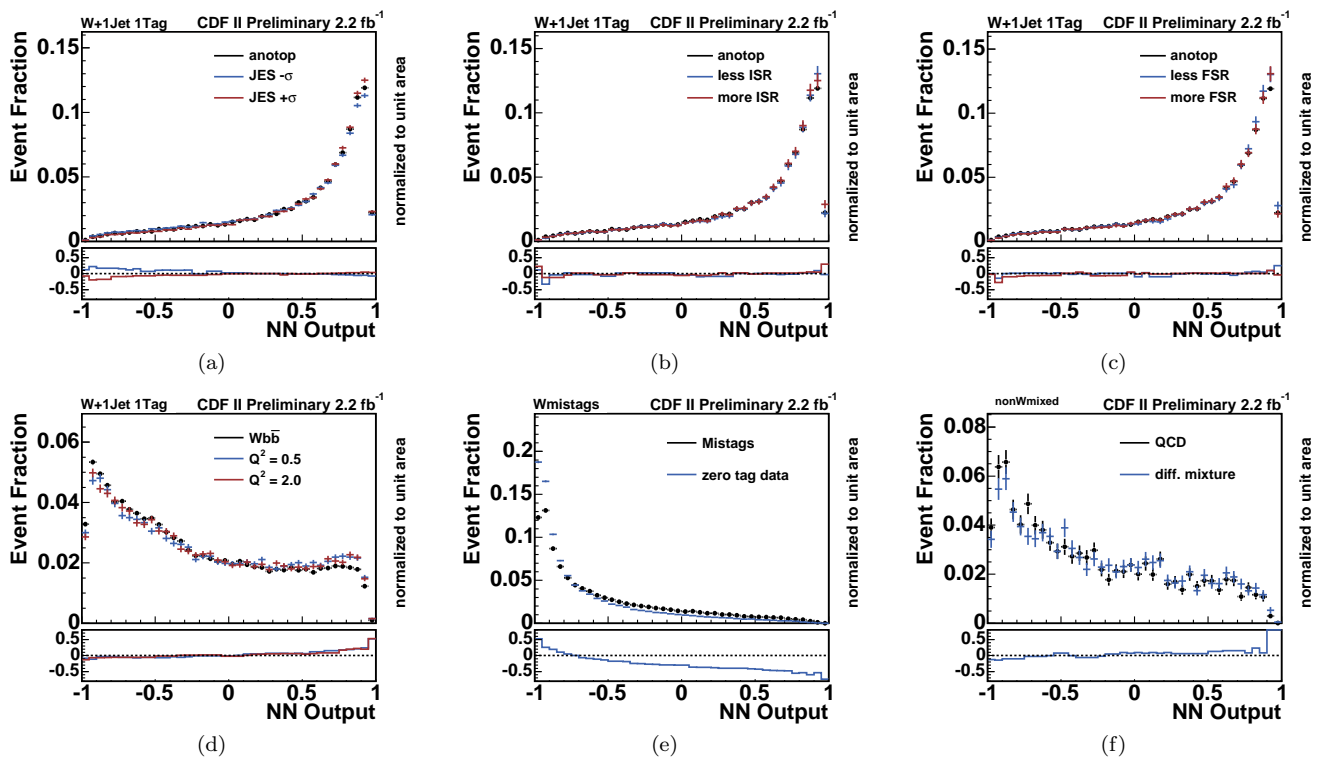


FIG. 3: Shape systematics due to the uncertainty on the jet energy correction (a), initial (b) and final (c) state radiation for anomalous top-quark, due to the uncertainty in the ALPGEN factorization/renormalization scale Q^2 for the $Wb\bar{b}$ background(d) due to the influence of the mistag model (e) and due to the influence of the nonW flavor composition. In the upper row the default distribution is shown in comparison to the shifted one. In the lower row the relative difference between the shifted distribution and the default is plotted.

process	Δ
single-top	15.0 %
$t\bar{t}$	14.0 %
$Wb\bar{b} + Wc\bar{c}$	flat prior
Wc	30.0 %
Mistags	16.6 %
Z+jets	10.8 %
Diboson	10.0 %
QCD	40.0 %

TABLE IV: Cross section uncertainties.

upper limit of 1.4 pb obtained from ensemble tests. The probability to obtain an upper limit higher than the observed

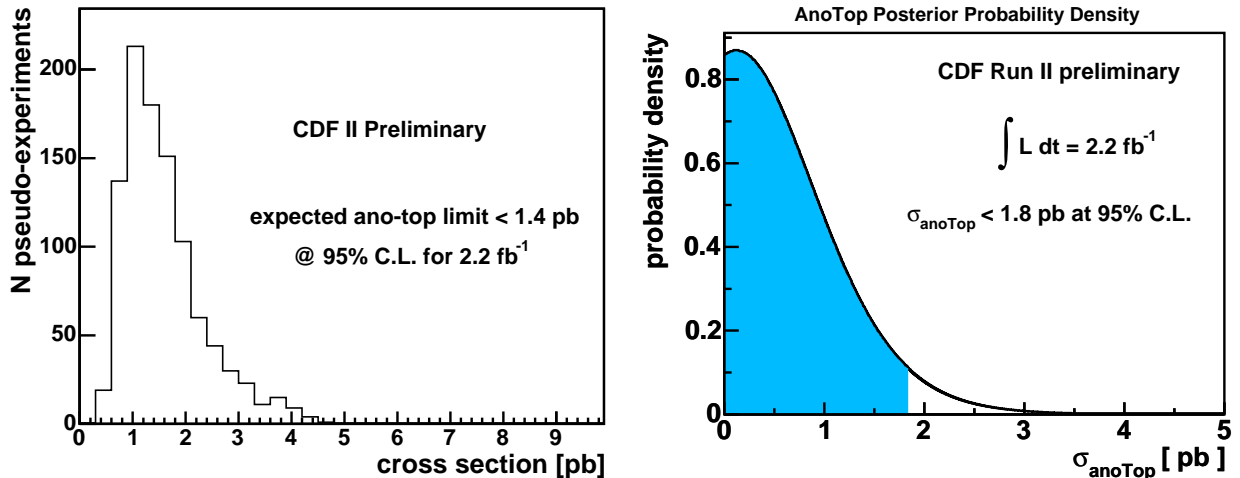


FIG. 4: Expected and observed limit on the anomalous top-quark cross section. (a) Expected limit, obtained from ensemble tests. (b) Observed limit, obtained from the fit to the $W + 1$ jet data sample.

1.8 pb under the assumption that FCNC top-quark production does not exist is 28%. Both limits are shown in Fig. 4.

VI. LIMITS ON THE FCNC COUPLING CONSTANTS

Using theoretical predictions of $\sigma(u(c) + g \rightarrow t)$ which include threshold resummation effects [32, 33], we convert the upper limit on the cross section into upper limits on the FCNC coupling constants (Fig. 5) at the 95% C.L. and find $\kappa_{gtu}/\Lambda < 0.018 \text{ TeV}^{-1}$, assuming $\kappa_{gtc} = 0$ and $\kappa_{gtc}/\Lambda < 0.069 \text{ TeV}^{-1}$, assuming $\kappa_{gtu} = 0$.

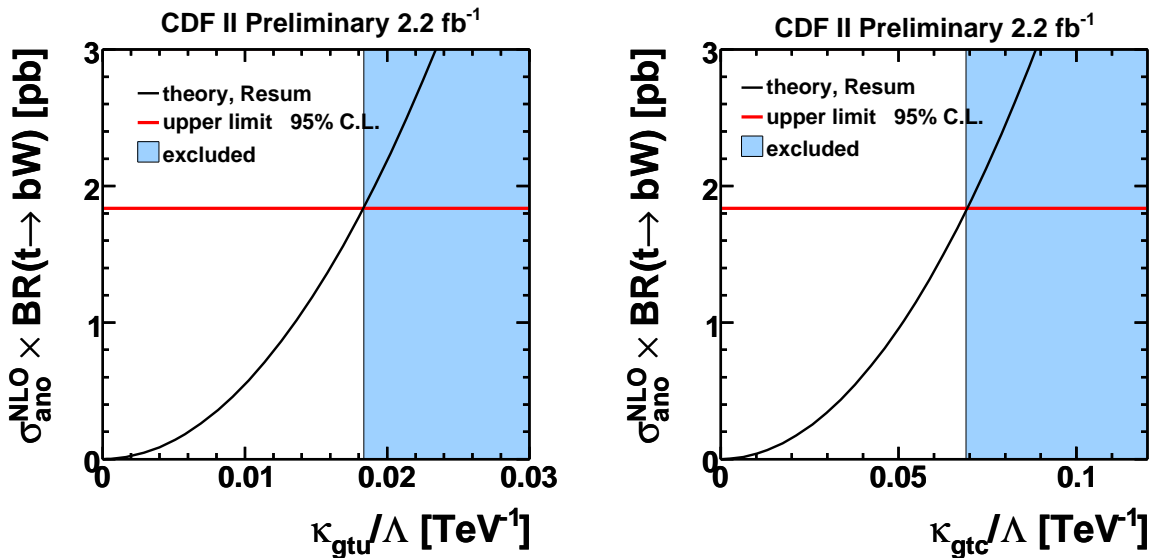


FIG. 5: Limits on the anomalous coupling constants as derived from the limit on the cross section. (a) Upper limit on the coupling constant $\frac{\kappa_{gtu}}{\Lambda}$. (b) Upper limit on the coupling constant $\frac{\kappa_{gtc}}{\Lambda}$. The composite model is compared to the distribution observed in collision data.

One can also express the limits on the coupling constants as limits on the FCNC branching ratios at leading order (Fig. 6) and obtains: $\text{BR}(t \rightarrow u + g) < 9.18 \times 10^{-4}$ and $\text{BR}(t \rightarrow c + g) < 1.73 \times 10^{-2}$.

In summary, we have explored the $W+1$ jet data set at CDF corresponding to an integrated luminosity of 2.2 fb^{-1} in search for single top-quarks produced by gluon-induced FCNC. No evidence for such processes are found, resulting

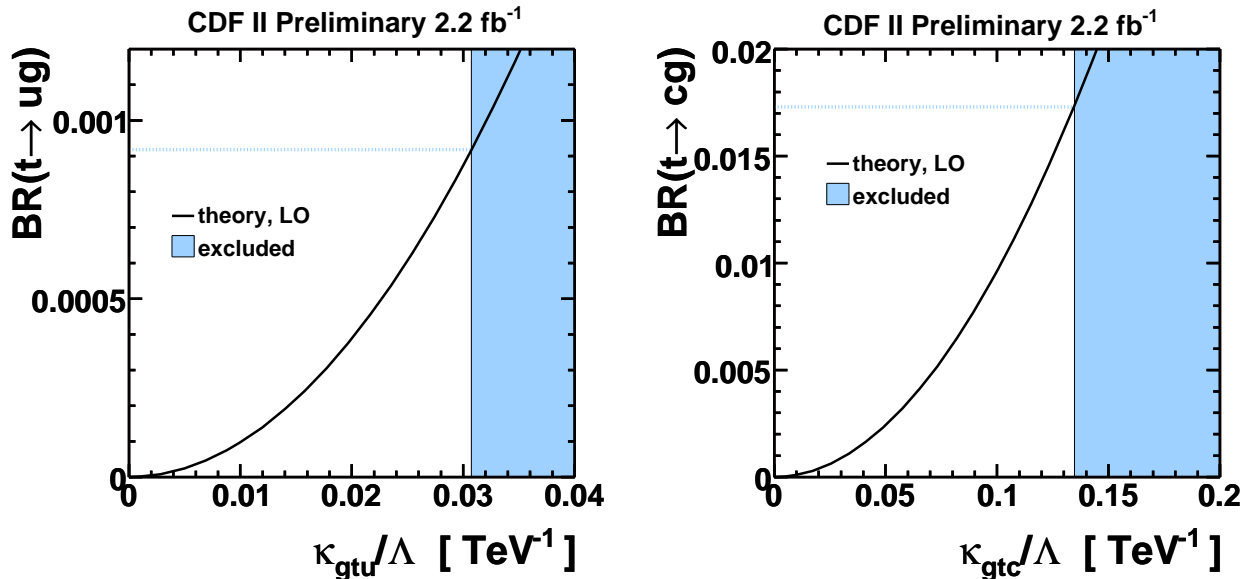


FIG. 6: Upper limit on the anomalous branching ratios. The black line is the theoretical trend (LO). The limits on the coupling constants in LO calculation are $\kappa_{gtu}/\Lambda < 0.031 \text{ TeV}^{-1}$ and $\kappa_{gtc}/\Lambda < 0.134 \text{ TeV}^{-1}$. The correspondent limits on the BRs are $BR(t \rightarrow ug) < 9.18 \times 10^{-4}$ and $BR(t \rightarrow cg) < 1.73 \times 10^{-2}$.

in the most stringent limits on the FCNC coupling constants κ_{gtu}/Λ and κ_{gtc}/Λ to date.

Acknowledgments

We thank the Fermilab staff and the technical staffs of the participating institutions for their vital contributions. This work was supported by the U.S. Department of Energy and National Science Foundation; the Italian Istituto Nazionale di Fisica Nucleare; the Ministry of Education, Culture, Sports, Science and Technology of Japan; the Natural Sciences and Engineering Research Council of Canada; the National Science Council of the Republic of China; the Swiss National Science Foundation; the A.P. Sloan Foundation; the Bundesministerium fuer Bildung und Forschung, Germany; the Korean Science and Engineering Foundation and the Korean Research Foundation; the Particle Physics and Astronomy Research Council and the Royal Society, UK; the Russian Foundation for Basic Research; the Comision Interministerial de Ciencia y Tecnologia, Spain; and in part by the European Community's Human Potential Programme under contract HPRN-CT-20002, Probe for New Physics.

-
- [1] S.L. Glashow, J. Iliopoulos, and L.Maiani, Phys. Rev. D **2**, 1285 (1970).
 - [2] G. Eilam, J.L. Hewett, and A. Soni, Phys. Rev. D **44**, 1473 (1991); Erratum: Phys. Rev. D **59**, 039901 (1999).
 - [3] B. Grzadkowski, J.F. Gunion, and P. Krawczyk, Phys. Lett. B **268**, 106 (1991).
 - [4] W.-S. Hou, Phys. Lett. B **296**, 179 (1992).
 - [5] G. Eilam *et al.*, Phys. Lett. B **510**, 227 (2001).
 - [6] J.M. Yang, B.-L. Young, and X. Zhang, Phys. Rev. D **58**, 055001 (1998).
 - [7] C. Yue *et al.*, Phys. Lett. B **508**, 290 (2001).
 - [8] E. Malkawi and T. Tait, Phys. Rev. D **54**, 5758 (1996).
 - [9] M. Hosch, K. Whisnant, and B.-L. Young, Phys. Rev. D **56**, 5725 (1997).
 - [10] A. Datta *et al.*, Phys. Rev. D **56**, 3107 (1997).
 - [11] T. Han *et al.*, Phys. Rev. D **58**, 073008 (1998).
 - [12] T.M.P. Tait and C.-P. Yuan, Phys. Rev. D **63**, 014018 (2000).
 - [13] V.M. Abazov *et al.* (DØ Collaboration), Phys. Rev. Lett. **99**, 191802 (2007).
 - [14] T. Aaltonen *et al.* (CDF Collaboration), public conference note no. 9202.
 - [15] P. Achard *et al.* (L3 Collaboration), Phys. Lett. B **549**, 290 (2002).

- [16] S. Chekanov *et al.* (ZEUS Collaboration), Phys. Lett. B **559**, 153.
- [17] A. Aktas *et al.* (H1 Collaboration), Eur. Phys. J. C **33**, 9 (2004).
- [18] D. Acosta *et al.* (CDF Collaboration), Phys. Rev. **D71**, 032001 (2005).
- [19] The \cancel{E}_T vector is corrected for the energy deposition of the high-energy muons as well as for the jet energy corrections.
- [20] A. Bhatti *et al.*, Nucl. Instrum. Methods, **A566**, 2 (2006).
- [21] D. Acosta *et al.*, Phys. Rev. **D71**, 052003 (2005).
- [22] T. Aaltonen *et al.*, CDF public note no. 9251.
- [23] T. Sjöstrand *et al.*, Comput. Phys. Commun **135**, 238 (2001).
- [24] J.M. Campbell and R.K. Ellis, Phys. Rev. **D60**, 113006, (1999).
- [25] R. Bonciani *et al.*, Nucl. Phys. **B529**, 424 (1998); M. Cacciari *et al.*, J. High Energy Phys. **0404**, 068 (2004).
- [26] J. Alwall *et al.*, J. High Energy Phys. **0709** 028 (2007).
- [27] B. W. Harris *et al.*, Phys. Rev. **D66**, 054024 (2004); Z. Sullivan, Phys. Rev. **D70**, 114012 (2004).
- [28] M. L. Mangano *et al.*, J. High Energy Phys **0307**, 001 (2003); M. L. Mangano *et al.*, Nucl. Phys. **B632** 343 (2002); F. Caravaglios *et al.*, Nucl. Phys. **B539** 215 (1999).
- [29] S.R. Slabospitsky and L. Sonnenschein, Comput. Phys. Commun. **148**, 87 (2002).
- [30] M. Feindt and U. Kerzel, Nucl. Instrum. Methods A **559**, 190-194 (2006).
- [31] S. Richter, Ph.D. thesis, University of Karlsruhe (2007), FERMILAB-THESIS-2007-35 (2007).
- [32] J.J. Liu, C.S. Li, L.L. Yang, and L.G. Jin, Phys. Rev. D **72**, 074018 (2005).
- [33] L.L. Yang *et al.*, Phys. Rev. D **73**, 074017 (2006).